

The Resistance of the Inui S-201 Hull

Copyright © Ulrich Remmlinger, Germany, April 2014, revised August 2014

Abstract. The towing tank results of the Inui-hulls are well suited for a validation of computer simulations and prediction methods of the wave resistance of ships. The original data is presented in a new form with the necessary corrections applied.

NOMENCLATURE

| | | | |
|-----------|--|--------|--|
| A_{wet} | Wetted area of canoe body | Re | Reynolds number $U \cdot L_{WL} / \nu$ |
| Fn | Froude number $U / (g \cdot L_{WL})^{1/2}$ | U | Ship speed |
| g | gravitational acceleration = 9.81 m/s ² | ρ | Density of the water |
| L_{WL} | Length of the water line at rest | ν | Kinematic viscosity of the water |
| R | Resistance force | | |

1. INTRODUCTION

There are many different and competing ways to estimate the wave resistance of a ship. Any computer simulation program or other prediction method needs to be validated against reliable experimental results. Inui's tank test results [1] are well suited for this purpose. The quality of the originally published data can be slightly improved by applying a few corrections.

2. THE VISCOUS RESISTANCE

Inui conducted experiments with a submerged double model in the towing tank and presented the results in a diagram. The measurement points were taken from this diagram and corrected for the blockage effect following Tamura's method [2]. The number of turbulence generators was estimated from Inui's description to be 23 in the first row and 31 in the second. The increment in the drag coefficient caused by these protrusions varies between $8 \cdot 10^5$ and $1 \cdot 10^4$, depending on the boundary layer thickness [3]. This error was subtracted from the measured friction coefficients. The corrected test results are depicted in figure 1.

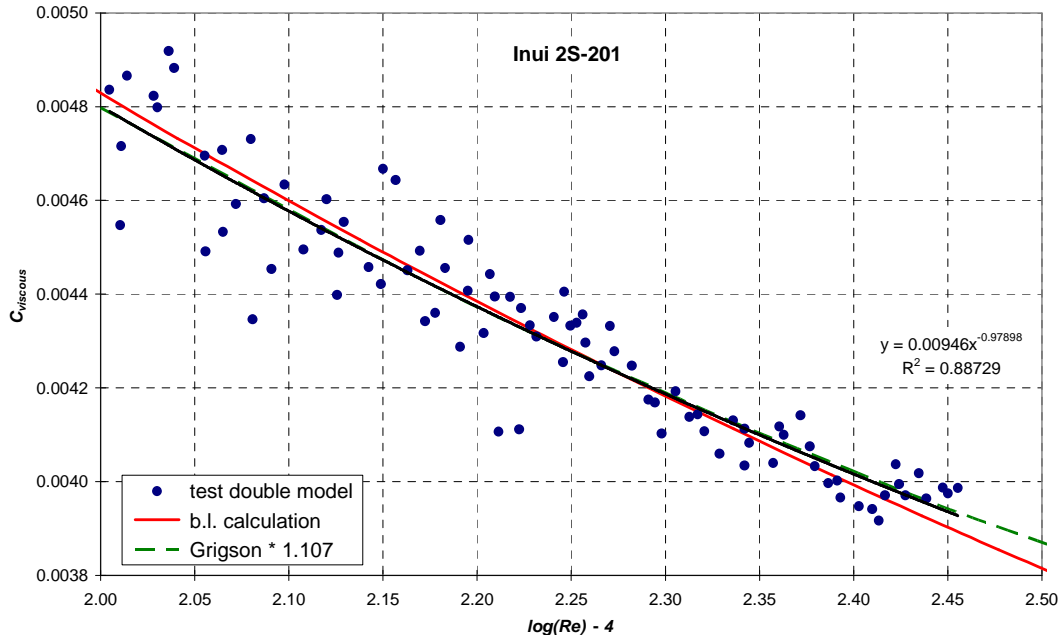


Figure 1. Viscous resistance coefficient of S-201 from double model measurements

A least squares regression of the test points (black line) gave the best fit for the following equation:

$$C_{visc} = \frac{R_{visc}}{\frac{1}{2} \cdot \rho \cdot U^2 \cdot A_{wet}} = \frac{0.00946}{(\log(Re) - 4.)^{0.979}} \quad (1)$$

This equation includes the form factor and is only valid for this specific hull. For comparison Grigson's correlation line is added. If multiplied with a form factor of 1.107, the agreement is exact. The red line is the result of a boundary layer calculation described in [4]. No assumption of a form factor is needed for the b.l. calculation. Only the turbulence level of 1.5 % was chosen. All three lines agree quite well and establish some confidence in the test results in spite of the large scatter of the experimental points.

3. THE RESIDUARY RESISTANCE

The difference between the measured total resistance and the viscous resistance is the residuary resistance. The viscous resistance was calculated from equation (1), increased by the drag of the turbulence generators. For the residuary resistance component an additional correction had to be applied [2] due to the limited depth of the tank. The resulting 115 data points were sorted and 4 outliers were removed. After that the curve was smoothed by averaging each two neighboring points. The result is shown in figure 2. The coefficients are valid for the clean hull without turbulence generators.

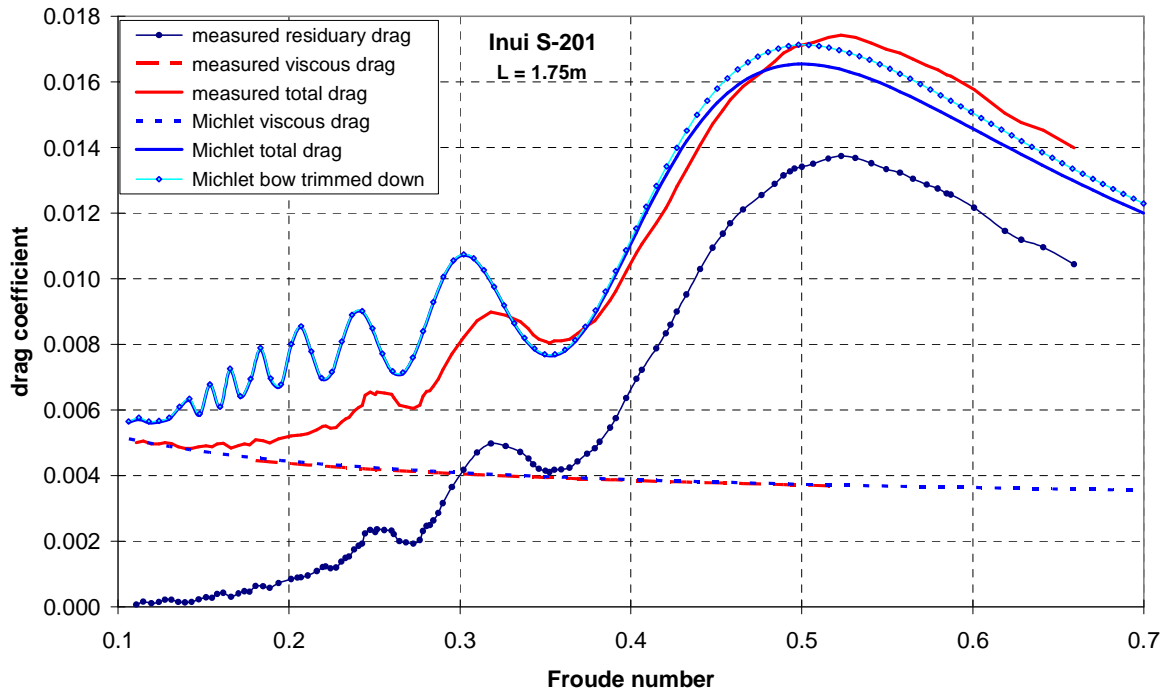


Figure 2. Calculated and measured drag coefficients for S-201

The numerical results are listed in table 1 at the end of this paper as a database for validation purposes.

4. COMPARISON WITH MICHLET

With a length to beam ratio of 8.1 it seems possible to use Michell's thin ship theory for the prediction of the wave resistance. The curves in figure 2 were calculated with the program Michlet [5]. The setting in the input file for the computation of the viscous resistance was Grigson's line with a form factor of 1.107. Above $Fn = 0.35$ the prediction is good. The half entrance angle of the hull S-201 is 21degrees, which might be too large for the short waves below $Fn = 0.35$.

During the experiments the model was suspended in the carriage in such a way that it was free to heave but restricted in pitch. A trim angle of zero degrees was maintained throughout the tests. At higher speeds this is only possible if the towing mechanism exerts a bow down trimming moment. If this bow down trim is added in the Michlet simulation, the agreement with the prediction improves at the high speeds.

What is also visible in figure 2 is a phase shift between the measured and the predicted values. The maximum drag coefficient is reached in the experiments at higher Froude numbers than in the simulation. A similar phase shift is known from experiments with geosims of Wigley hulls. Kajitani et al. [6] report experimental results for models of 2, 2.5, 4 and 6 meters length. The smaller the model the more are the humps and hollows shifted towards higher Froude numbers. It seems that the viscous wake extends the "effective" length of the model and

smaller models have a larger boundary layer thickness relative to their length. From b.l. theory it is known that the turbulent b.l. thickness on a flat plate with the length of L_{WL} is approximately $0.37 \cdot L_{WL} \cdot Re^{-0.2}$. Assuming that the additional length of the wake is proportional to this b.l. thickness one can define an "effective" Froude number:

$$Fn_{effective} = \frac{U}{\sqrt{g \cdot L_{WL} \cdot (1 + C \cdot Re^{-0.2})}} \quad (2)$$

A constant factor of $C = 0.7$ is chosen for the curve in figure 3. The agreement at higher speeds is remarkable.

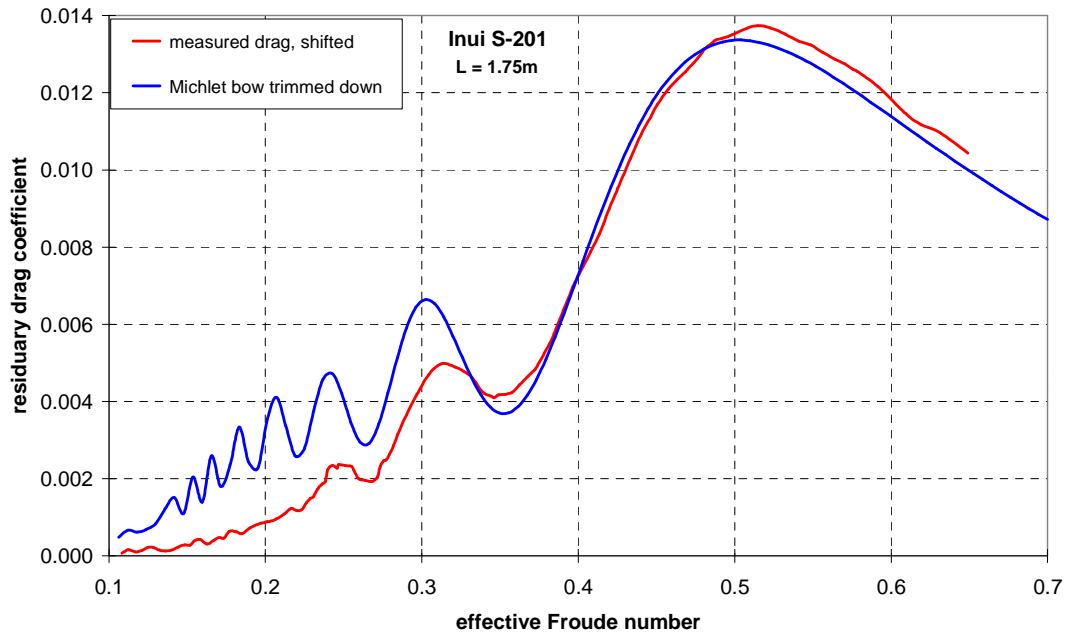


Figure 3. Calculated and measured residuary drag coefficients with phase shift

5. REFERENCES

1. Inui, T., "Study on Wave-Making Resistance of Ships", in *60th Anniversary Series Vol. 2, Advances in Calculation of Wave-Making Resistance of Ships*, Inui and Maruo Eds., Tokyo, Japan: The Society of Naval Architects of Japan, 1957, pp. 173-355
2. Tamura, K., "Study on the Blockage Correction", *Journal Society Naval Architects Japan*, Vol. 131, 1972, pp. 17-28
3. Hoerner, S.F., *Fluid-Dynamic Drag*, Midland Park, NJ, 1965
4. Remmlinger, U., "The Influence of Sand Grain Strips on Boundary Layer Transition in the Towing Tank", [Online]. Available: www.remmlinger.com/B-L-trip.pdf
5. Lazauskas, L.V., [Online]. Available: www.cyberiad.net
6. Kajitani, Miyata, Ikehata, Tanaka, Adachi, Namimatsu, Ogiwara, "The Summary of the Cooperative Experiment on Wigley Parabolic Model in Japan", Tokyo University, Japan, 1983

6. APPENDIX

| F_n | Re | $C_{residuary}$ | $C_{viscous}$ |
|--------|-----------|-----------------|---------------|
| 0.1107 | 9.123E+05 | 0.00007 | 0.00490 |
| 0.1147 | 9.452E+05 | 0.00016 | 0.00486 |
| 0.1195 | 9.850E+05 | 0.00011 | 0.00482 |
| 0.1239 | 1.021E+06 | 0.00014 | 0.00478 |
| 0.1275 | 1.051E+06 | 0.00022 | 0.00475 |
| 0.1312 | 1.082E+06 | 0.00022 | 0.00472 |
| 0.1352 | 1.114E+06 | 0.00015 | 0.00469 |
| 0.1391 | 1.146E+06 | 0.00013 | 0.00467 |
| 0.1431 | 1.179E+06 | 0.00015 | 0.00464 |
| 0.1472 | 1.213E+06 | 0.00023 | 0.00461 |
| 0.1515 | 1.249E+06 | 0.00029 | 0.00458 |
| 0.1549 | 1.277E+06 | 0.00028 | 0.00456 |
| 0.1579 | 1.302E+06 | 0.00039 | 0.00455 |
| 0.1616 | 1.332E+06 | 0.00042 | 0.00453 |
| 0.1662 | 1.369E+06 | 0.00030 | 0.00450 |
| 0.1705 | 1.405E+06 | 0.00041 | 0.00448 |
| 0.1739 | 1.433E+06 | 0.00047 | 0.00446 |
| 0.1769 | 1.458E+06 | 0.00046 | 0.00444 |
| 0.1804 | 1.487E+06 | 0.00063 | 0.00443 |
| 0.1848 | 1.523E+06 | 0.00063 | 0.00441 |
| 0.1888 | 1.556E+06 | 0.00057 | 0.00439 |
| 0.1938 | 1.598E+06 | 0.00073 | 0.00437 |
| 0.2012 | 1.658E+06 | 0.00085 | 0.00434 |
| 0.2049 | 1.689E+06 | 0.00088 | 0.00432 |
| 0.2057 | 1.695E+06 | 0.00090 | 0.00431 |
| 0.2057 | 1.695E+06 | 0.00095 | 0.00430 |
| 0.2057 | 1.695E+06 | 0.00109 | 0.00428 |
| 0.2057 | 1.695E+06 | 0.00121 | 0.00426 |
| 0.2140 | 1.764E+06 | 0.00123 | 0.00426 |
| 0.2243 | 1.849E+06 | 0.00117 | 0.00425 |
| 0.2275 | 1.875E+06 | 0.00120 | 0.00424 |
| 0.2306 | 1.900E+06 | 0.00138 | 0.00422 |
| 0.2330 | 1.920E+06 | 0.00149 | 0.00422 |
| 0.2350 | 1.937E+06 | 0.00153 | 0.00421 |
| 0.2381 | 1.962E+06 | 0.00175 | 0.00420 |
| 0.2407 | 1.984E+06 | 0.00186 | 0.00419 |
| 0.2428 | 2.001E+06 | 0.00192 | 0.00418 |
| 0.2445 | 2.015E+06 | 0.00224 | 0.00418 |
| 0.2475 | 2.040E+06 | 0.00234 | 0.00417 |
| 0.2505 | 2.065E+06 | 0.00228 | 0.00416 |
| 0.2515 | 2.073E+06 | 0.00236 | 0.00416 |
| 0.2557 | 2.108E+06 | 0.00234 | 0.00414 |
| 0.2599 | 2.142E+06 | 0.00232 | 0.00413 |
| 0.2614 | 2.154E+06 | 0.00221 | 0.00413 |
| 0.2645 | 2.180E+06 | 0.00200 | 0.00412 |
| 0.2685 | 2.213E+06 | 0.00196 | 0.00411 |
| 0.2727 | 2.248E+06 | 0.00193 | 0.00410 |
| 0.2765 | 2.279E+06 | 0.00203 | 0.00409 |
| 0.2783 | 2.294E+06 | 0.00231 | 0.00408 |
| 0.2805 | 2.312E+06 | 0.00246 | 0.00408 |
| 0.2824 | 2.328E+06 | 0.00249 | 0.00407 |
| 0.2845 | 2.345E+06 | 0.00263 | 0.00407 |
| 0.2873 | 2.368E+06 | 0.00286 | 0.00406 |
| 0.2899 | 2.390E+06 | 0.00315 | 0.00405 |
| 0.2954 | 2.434E+06 | 0.00365 | 0.00404 |
| 0.3021 | 2.490E+06 | 0.00417 | 0.00402 |

| | | | |
|--------|-----------|---------|---------|
| 0.3100 | 2.555E+06 | 0.00470 | 0.00400 |
| 0.3182 | 2.623E+06 | 0.00498 | 0.00399 |
| 0.3268 | 2.693E+06 | 0.00490 | 0.00397 |
| 0.3352 | 2.763E+06 | 0.00472 | 0.00395 |
| 0.3401 | 2.803E+06 | 0.00452 | 0.00394 |
| 0.3429 | 2.826E+06 | 0.00434 | 0.00393 |
| 0.3461 | 2.853E+06 | 0.00421 | 0.00393 |
| 0.3501 | 2.886E+06 | 0.00414 | 0.00392 |
| 0.3524 | 2.905E+06 | 0.00410 | 0.00392 |
| 0.3552 | 2.928E+06 | 0.00417 | 0.00391 |
| 0.3593 | 2.961E+06 | 0.00418 | 0.00390 |
| 0.3641 | 3.001E+06 | 0.00424 | 0.00389 |
| 0.3687 | 3.039E+06 | 0.00443 | 0.00388 |
| 0.3744 | 3.086E+06 | 0.00467 | 0.00387 |
| 0.3789 | 3.123E+06 | 0.00483 | 0.00387 |
| 0.3818 | 3.147E+06 | 0.00503 | 0.00386 |
| 0.3878 | 3.197E+06 | 0.00546 | 0.00385 |
| 0.3912 | 3.224E+06 | 0.00575 | 0.00385 |
| 0.3973 | 3.274E+06 | 0.00636 | 0.00384 |
| 0.4032 | 3.323E+06 | 0.00695 | 0.00383 |
| 0.4065 | 3.350E+06 | 0.00722 | 0.00382 |
| 0.4148 | 3.419E+06 | 0.00788 | 0.00381 |
| 0.4205 | 3.466E+06 | 0.00834 | 0.00380 |
| 0.4231 | 3.488E+06 | 0.00860 | 0.00380 |
| 0.4269 | 3.519E+06 | 0.00900 | 0.00379 |
| 0.4325 | 3.564E+06 | 0.00952 | 0.00378 |
| 0.4406 | 3.631E+06 | 0.01029 | 0.00377 |
| 0.4478 | 3.691E+06 | 0.01095 | 0.00376 |
| 0.4539 | 3.741E+06 | 0.01137 | 0.00375 |
| 0.4581 | 3.776E+06 | 0.01169 | 0.00375 |
| 0.4656 | 3.838E+06 | 0.01211 | 0.00374 |
| 0.4764 | 3.926E+06 | 0.01255 | 0.00372 |
| 0.4841 | 3.990E+06 | 0.01289 | 0.00371 |
| 0.4893 | 4.033E+06 | 0.01315 | 0.00371 |
| 0.4931 | 4.064E+06 | 0.01327 | 0.00370 |
| 0.4958 | 4.086E+06 | 0.01336 | 0.00370 |
| 0.5001 | 4.122E+06 | 0.01341 | 0.00369 |
| 0.5067 | 4.176E+06 | 0.01350 | 0.00368 |
| 0.5156 | 4.250E+06 | 0.01367 | 0.00367 |
| 0.5230 | 4.311E+06 | 0.01374 | 0.00367 |
| 0.5313 | 4.379E+06 | 0.01368 | 0.00366 |
| 0.5407 | 4.457E+06 | 0.01352 | 0.00365 |
| 0.5495 | 4.529E+06 | 0.01334 | 0.00364 |
| 0.5575 | 4.595E+06 | 0.01324 | 0.00363 |
| 0.5650 | 4.657E+06 | 0.01305 | 0.00362 |
| 0.5732 | 4.724E+06 | 0.01287 | 0.00361 |
| 0.5795 | 4.776E+06 | 0.01275 | 0.00361 |
| 0.5847 | 4.820E+06 | 0.01260 | 0.00360 |
| 0.5872 | 4.840E+06 | 0.01256 | 0.00360 |
| 0.6009 | 4.952E+06 | 0.01216 | 0.00359 |
| 0.6188 | 5.101E+06 | 0.01146 | 0.00357 |
| 0.6284 | 5.179E+06 | 0.01119 | 0.00356 |
| 0.6412 | 5.285E+06 | 0.01096 | 0.00355 |
| 0.6592 | 5.434E+06 | 0.01044 | 0.00353 |

Table1. Corrected values for S-201